Journal of Magnetism and Magnetic Materials 545 (2022) 168769

Contents lists available at ScienceDirect

Journal of Magnetism and Magnetic Materials

journal homepage: www.elsevier.com/locate/jmmm

Tuning magnetocaloric effect of Gd-Co-Al-Si bulk metallic glass via controlling degree of structural order

Zhengguo Zhang [a], Qiang Luo [a,*], Liliang Shao [a], Lin Xue [a], Bo Chen [b,c], Baolong Shen [a,d,*]

[a] School of Materials Science and Engineering, Jiangsu Key Laboratory for Advanced Metallic Materials, Southeast University, Nanjing 211189, China
[b] School of Materials Science and Engineering, Tongji University, Shanghai 201804, China
[c] Key Laboratory of Advanced Civil Engineering Materials (Tongji University), Ministry of Education, Shanghai 201804, China
[d] Institute of Massive Amorphous Metal Science, China University of Mining and Technology, Xuzhou 221116, China

ARTICLE INFO

Keywords:
Structural order
Magnetocaloric effect
Metallic glasses
Crystallization enthalpy

ABSTRACT

The influence of degree of structural order tuned by annealing on magnetocaloric properties of $Gd_{55}Co_{20}Al_{24.5}Si_{0.5}$ bulk metallic glass (MG) was investigated. It is uncovered that moderate enhancement of structural order can increase the magnetocaloric effect (MCE), but excessive degree of structural order reduces the MCE. Through tuning the degree of structural order, the maximum magnetic entropy change of the MG annealed at 536 K for 60 min reaches 10.8 ± 0.6 $JKg^{-1}K^{-1}$ under 5 T, which is the highest value of the Gd-based MGs, indicating the promising prospect of these alloys as magnetic refrigerant candidates. Besides, it's found that the degree of structural order, reflected by the crystallization enthalpy change, and the magnetic entropy change have a good linear correspondence, which sheds new light on the nature of MCE in MGs and is of significance to the design of novel amorphous magnetic refrigerants.

During the past decades, the magnetocaloric properties of magnetic solids have gained considerable attention in both academia and engineering [1–10]. Among them the metallic glasses are promising magnetic refrigerant due to their many beneficial features, such as high resistance, low eddy current loss, low coercivity, and large refrigerant capacity [11–13]. And great efforts have been devoted to achieving large or giant magnetocaloric effect (MCE) by developing new alloy system, irradiation, hydrogenation and making alloys into composite, *etc* [14–19]. However, the interplay between structure and magnetocaloric properties is not well understood until now in MGs because of the disordered and heterogeneous nature [20–23].

MGs are generally prepared by rapid cooling of a high-temperature melt, and thus are intrinsic unstable or metastable in nature. Therefore, heat treatment can change easily the disordered structure and energy state of the system, causing it to relax to a more stable glassy state with higher degree of structural order or crystallize (after annealing below or above crystallization temperature, T_x). Tuning structural order of MGs through annealing has been widely used to adjust mechanical properties of Zr-based MGs and soft magnetic performance of Fe-based MGs [24,25]. Some researches about the effect of crystallization on magnetocaloric property of MGs have also been reported, which find that crystallization usually reduces the MCE [26,27]. In a few investigations, table-like feature or enhancement of MCE after partial crystallization was obtained due to formation of some metastable intermediate phases [28–30]. In addition, little or slightly beneficial effects of annealing below glass transition temperature (T_g) on MCE were also observed in a few MG systems [30,31]. However, the correlation between degree of structural order and MCE is still rather elusive in MGs, which is hindering the development of amorphous magnetic cooling refrigerant.

In this paper, the influence of degree of structural order on magnetocaloric performance of $Gd_{55}Co_{20}Al_{24.5}Si_{0.5}$ bulk MG with excellent glass forming ability was explored [32]. We prepared alloys with different degrees of structural order and heterogeneity, remaining the complete amorphous structure, by controlling the isothermal annealing temperature (below T_x) and time. It is found that moderately enhanced degree of structural order can increase the MCE, but excessive degree of structural order reduces the MCE, indicating the existence of an optimal degree of structural order for achieving optimal MCE for a given MG. By tuning the degree of structural order, a maximum magnetic entropy change of 10.8 ± 0.6 $JKg^{-1}K^{-1}$ under 5 T has been obtained, which is the highest value of the Gd-based MGs reported. Moreover, a nearly linear

* Corresponding authors at: School of Materials Science and Engineering, Jiangsu Key Laboratory for Advanced Metallic Materials, Southeast University, Nanjing 211189, China (B. Shen).
E-mail addresses: q.luo@seu.edu.cn (Q. Luo), blshen@seu.edu.cn (B. Shen).

https://doi.org/10.1016/j.jmmm.2021.168769
Received 10 February 2021; Received in revised form 2 November 2021; Accepted 3 November 2021
Available online 9 November 2021

correlation between the degree of structural order and MCE is observed. These findings are of importance to develop advanced MG and related composite systems with excellent MCE.

The alloy ingot with nominal composition of $Gd_{55}Co_{20}Al_{24.5}Si_{0.5}$ was prepared by arc-melting Gd (99.9%), Co (99.99%), Al (99.99%) and Si (99.99%) under a Ti-gettered purified argon atmosphere. The ingot was repeatedly melted five times to obtain good chemical homogeneity and then was sucked into copper mold under a high-purity argon atmosphere to get a cylindrical rod with 2 mm in diameter and about 70 mm in length. At last, 8 wafer samples with the thickness of 1 mm were cut from the same cylindrical rod to minimize the error of experimental results. Isothermal annealing was carried out in Al_2O_3 pans by using differential scanning calorimeter (DSC, NETZSCH DSC 404F3) under flowing high purity argon. The microstructure of the alloys was investigated by X-ray diffraction (XRD, rigaku smartlab) with Cu Kα radiation with a scan rate of 2°/min and high-resolution transmission electron microscopy (HRTEM, FEI Tecnai G2F20). The magnetocaloric properties were investigated by a SQUID magnetometer (MPMS, Quantum Design SQUID-VSM). Vickers hardness (H_v) is the average of eight measurements by the Vickers micro-hardness tester (FM-700, FUTURE-TECH) under a load of 4.9 N.

To tune the degree of structural order, seven groups of samples were annealed at different temperatures around T_g (596 K) for different time intervals: 536 K ~ 0.9 T_g (60 min), 578 K ~ 0.97T_g (60 min) and 620 K ~ 1.04 T_g (30, 35, 40, 50 and 60 min), respectively. As presented in Fig. 1(a), the XRD patterns of all the as-cast and annealed MGs exhibit broad diffused peaks and no obvious sharp peak corresponding to crystallization phase, which indicates the outstanding thermal stability. In addition, note that the diffraction peak around 32° of the alloy annealed at 620 K for 60 min is sharper than that of the others, which indicates its most ordered local structure. Fig. 1(b) presents the DSC curves of the as-cast and annealed MGs measured at a heating rate of 40 K/min. It can be seen clearly that all the annealed MGs show clear glass transition and crystallization events, and both the height of the crystallization peak and crystallization enthalpies (the inset) decrease gradually with increasing annealing temperature and/or time. This indicates that the degree of structural order of the MG increases gradually upon annealing.

The HRTEM patterns of three typical alloys are shown in Fig. 2(a-c) to reveal more deeply the structural changes after annealing. At first sight, all the patterns look similar, irregular and maze-like, exhibiting typical amorphous feature without any nanocrystal, which agrees with the XRD results. However, some slight difference can be observed in the corresponding selected area electron diffraction (SAED) patterns (the insets). The halo ring becomes thinner for the MG annealed at 578 K for 60 min than that of the as-cast MG, and more diffraction rings appear for the MG annealed at 620 K for 60 min. This implies that the local structure of the MGs becomes gradually ordered after annealing, creating more and more crystal-like clusters as precursors of crystallization. The Reduce Density Function (RDF) curves calculated from the SAED patterns are shown in Fig. 2(d) [33], all of which have three peaks (marked as P_1, P_2, P_3, respectively). Fig. 2(e-f) compares the positions (Q) and full width at half maximums of the three peaks. It can be seen that all the peaks move to lower values with increasing annealing temperature, which means the alloy becomes denser and denser. Furthermore, the P_1 gradually becomes wider after annealing, while the P_2 and P_3 gradually become narrowed. This may reveal that the short-range-order clusters become more crystal-like and the medium-range-order structures become more heterogeneous. In addition, a shallow bulge at 7.5 nm^{-1} in the RDF curve of the as-cast MG disappears after annealing at 578 and 620 K for 60 min.

To estimate the area fraction of regions with local crystal-like order, the HRTEM image is divided into 144 square boxes with a length of 1.985 nm, which is similar to the typical size of local crystal-like order. And then the square sub-images are transformed into their 2D auto correlation images used to evaluate the structure translational symmetry [32,34–36], as shown in Fig. 2(g-i). For example, the sub-image located in the 5th row and 3rd column in Fig. 2(g) has an obvious symmetric fringe, thus we choose it as the demarcation to distinguish the local crystal-like order and disorder, and a square sub-image can be considered to be orderly when it shows clearer fringe than the demarcation one. As shown in Fig. 2(g-i), we analyzed all the square sub-images by the above method and marked the orderly sub-images by red frame. The area fractions of these crystal-like domains in the as-cast MG and the MGs annealed at 578 and 620 K for 60 min can be determined to be about 6.25%, 11.11% and 17.36%, respectively. It can be seen that the annealing increases obviously the degree of structural order, which agrees with the SAED results. In addition, in our measurement, we used high annealing temperatures (above 0.9T_g). Therefore, it is reasonable that medium range ordering processes dominates the relaxation [37]. The stress release should be of secondary importance on the magnetic behavior.

The annealing causes structure relaxation and local ordering through atom arrangement, which can result in the change of magnetic behaviors. Fig. 3 shows the change of field cooling magnetization (M) of the as-cast and annealed $Gd_{55}Co_{20}Al_{24.5}Si_{0.5}$ MGs at 0.05 T from 44 to 154 K. All the MGs show clearly a similar ferromagnetic-to-paramagnetic transition. As seen from the inset of Fig. 3, the Curie temperature (T_C), defined by the maximum of -dM/dT, decreases gradually (from 102 to 88 K) with the increase of annealing temperature and time.

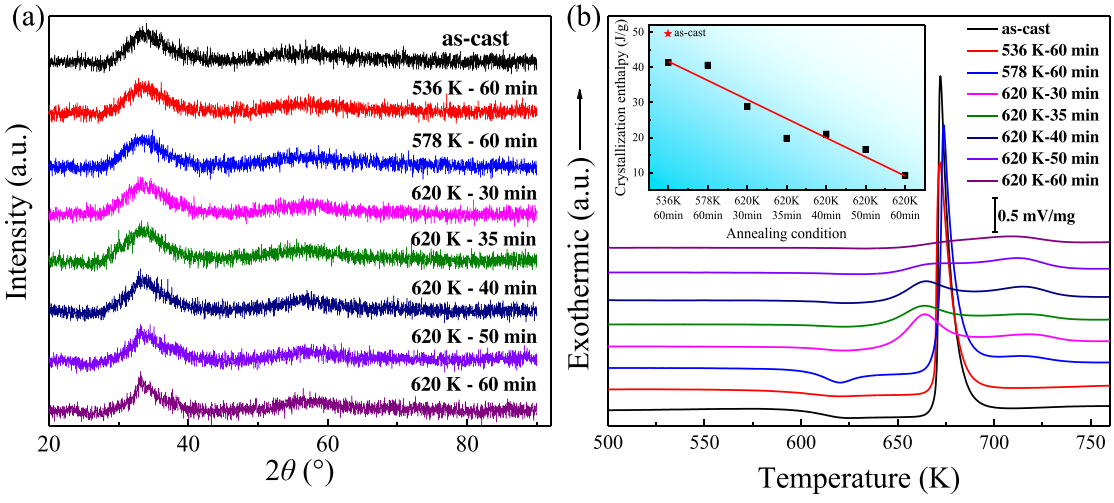

Fig. 1. (a) XRD patterns and (b) DSC curves of as-cast and annealed $Gd_{55}Co_{20}Al_{24.5}Si_{0.5}$ MGs, the inset shows the change of crystallization enthalpies.

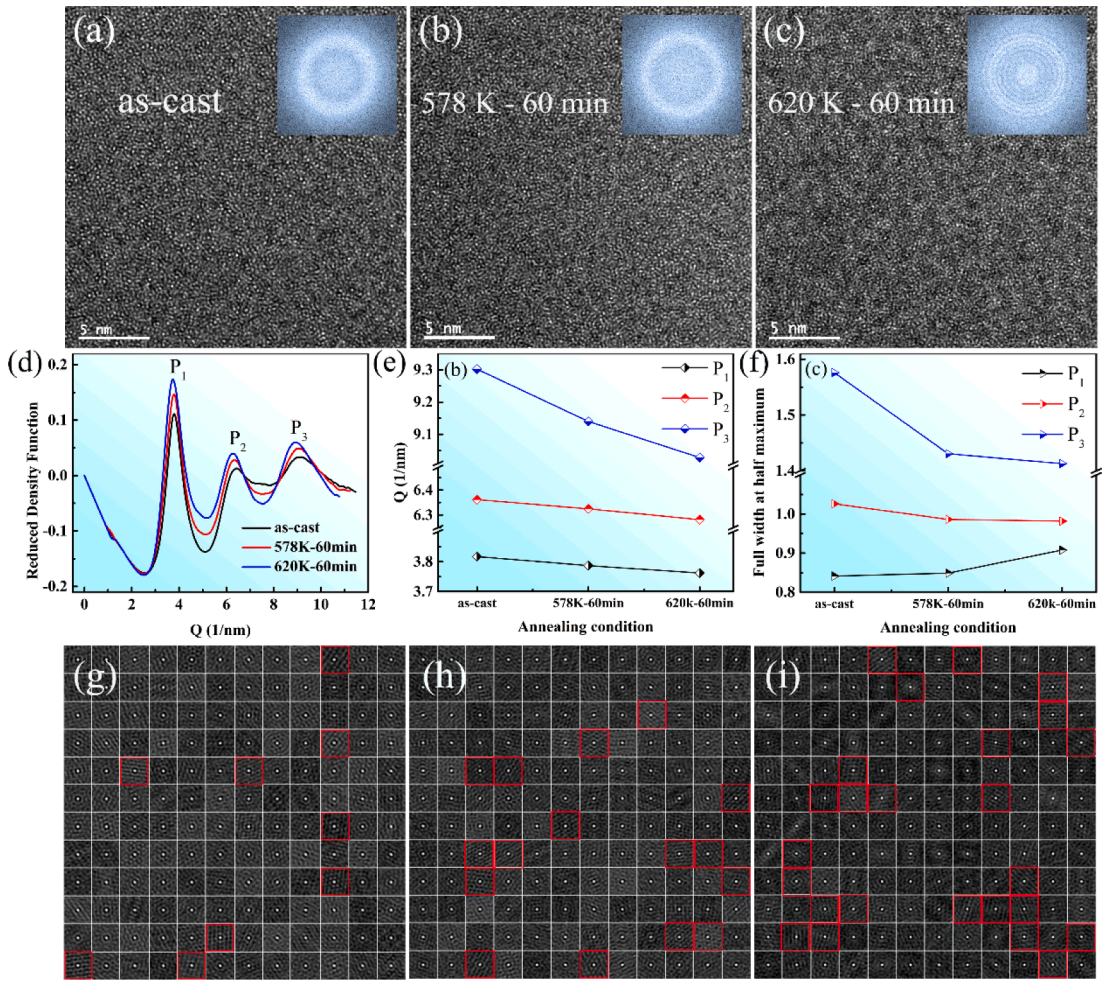

Fig. 2. (a-c) The HRTEM images of the as-cast MG and MGs annealed at 578 and 620 K for 60 min, the insets are corresponding SAED patterns. (d) The Reduce Density Function of the as-cast MG and MGs annealed at 578 and 620 K for 60 min. (e) the positions and (f) full width at half maximums of the three peaks. (g-i) The segmentation of the HRTEM images for auto-correlation analysis, the dimension of each sub-image is 1.985 × 1.985 nm^2.

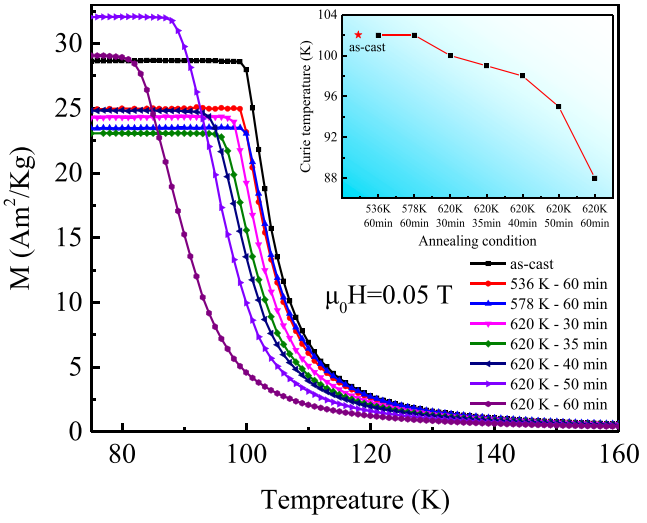

Fig. 3. The temperature dependence of field cooling magnetization of the as-cast and annealed MGs at 0.05 T, the insert shows the change of Curie temperature.

One set of typical isothermal M–H curves of the as-cast MG are shown in Fig. 4(a). Below T_C, the magnetization rises rapidly and approaches subsequently to saturation, different from the behavior above T_C. Fig. 4(b) compares the isothermal magnetization curves of all the as-cast and annealed MGs at 44 and 103 K. The saturation magnetization of the alloys has slight difference at the lowest temperature of 44 K, but it shows obvious and regular changes at 100 K (around T_C). Under 100 K, the magnetization of the two alloys annealed below T_g exceeds that of the as-cast alloy above certain magnetic field, below which there are almost the same. But all the other alloys annealed at 620 K (above T_g) show smaller magnetization than the as-cast alloy, and the magnetization decreases gradually with increasing annealing time. These results indicate that there are some differences between the ordering processes of short-to-medium range structures above and below T_g, which have different and complex impacts on the magnetic behavior. Magnetic entropy change ($-\Delta S_M$) can be calculated from the isothermal magnetization curves by using the thermodynamic Maxwell relation [38]. Fig. 4(c) shows the temperature dependent magnetic entropy changes under different magnetic fields for the as-cast MG. The $-\Delta S_M$ reaches its maximum at T_C, and all the other annealed MGs show similar temperature and field dependence of the magnetic entropy change. Usually, large saturation magnetization or sharp magnetic transition (large dM/dT) are beneficial to obtain large MCE. In order to find the main factor working here, we calculated the dM/dT values of these alloys. It is found that the variation trend of the maximum | dM/dT | with annealing condition does not match that of the MCE. On the other hand, the

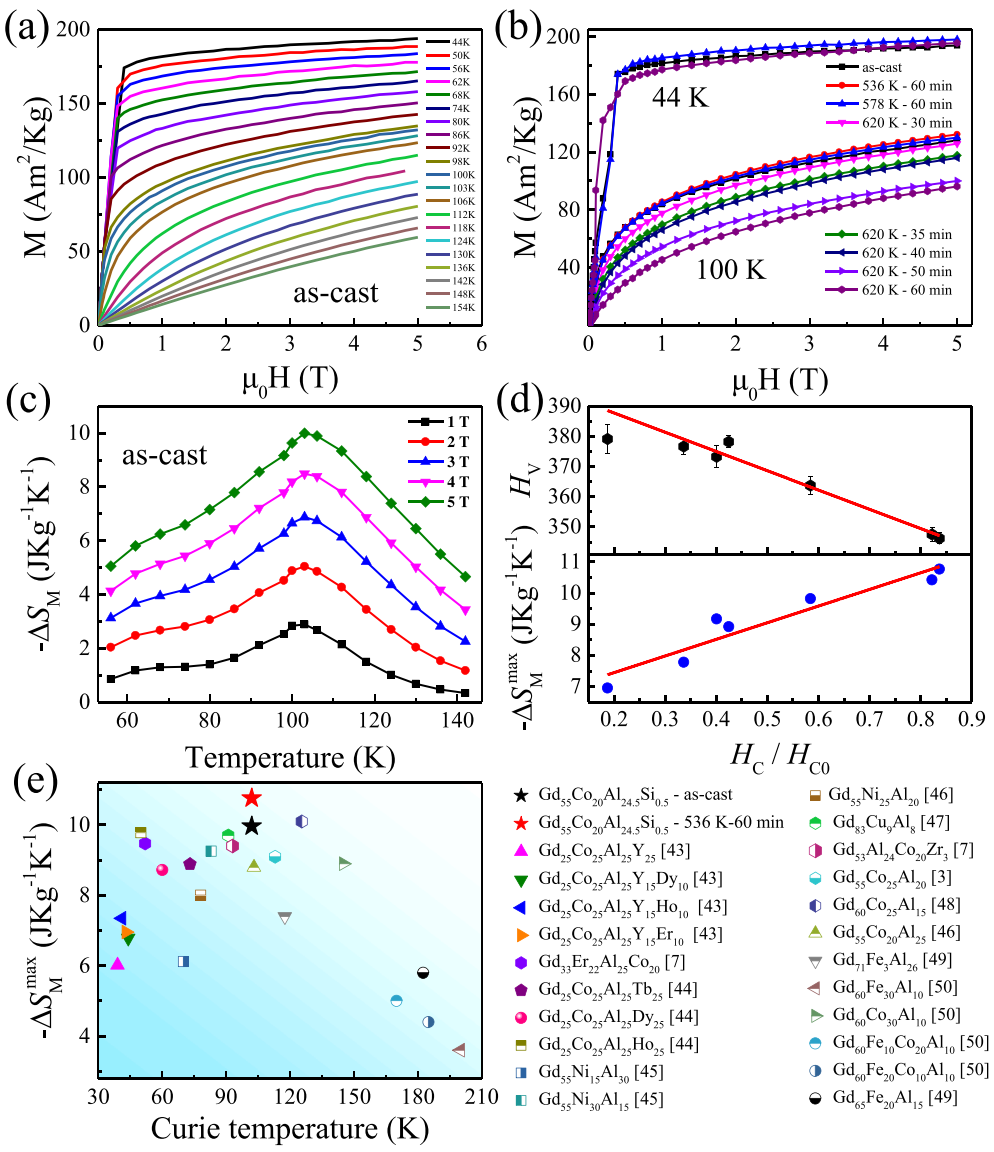

Fig. 4. (a) Isothermal magnetization curves of the as-cast MG. (b) Isothermal magnetization curves of the as-cast and annealed MGs at 44 and 103 K. (c) Magnetic entropy changes of the as-cast MG under different field changes. (d) The maximum magnetic entropy changes and Vickers hardness of the annealed MGs with different crystallization enthalpies. (e) Curie temperature and maximum magnetic entropy change of $Gd_{55}Co_{20}Al_{24.5}Si_{0.5}$ MG compared with those of other Gd-based MGs.

saturation magnetization as shown in Fig. 4(b) and maximum magnetic entropy change have the same variation trend with annealing condition. To uncover the effect of degree of structural order on the magnetocaloric properties, we calculate the ratio of crystallization enthalpy of the annealed MGs (H_C) to that of the as-cast MG (H_{C0}) and plot the H_C/H_{C0} dependence of the maximum magnetic entropy change ($-\Delta S_M^{max}$) under 5 T. Interestingly, a nearly linear relationship between $-\Delta S_M^{max}$ and H_C/H_{C0} (reflecting the degree of structural order) is observed for the annealed MGs as shown in Fig. 4 (d). Similar linear relationship is also obtained between Vickers hardness (H_v) and H_C/H_{C0}. The increase of H_v (from 340 to 380) with increasing structural order is due to the gradually increased density. Moreover, by tuning the degree of structural order, the $-\Delta S_M^{max}$ of present MG system can reach 10.8 ± 0.6 $JKg^{-1}K^{-1}$ after annealing at 536 K for 60 min, which is larger than the as-cast MG and other Gd-based MG systems reported in the literature as shown in Fig. 4 (e) [3,7,43–50]. Although the $-\Delta S_M^{max}$ increase of the sample annealed at 536 K for 60 min is comparable to (slightly larger than) the systematic error of 5 to 10%, the present results suggest an improvement in magnetic entropy change after annealing. The improvement of $-\Delta S_M^{max}$ may be due to the denser structure and enhanced exchange interaction by the formation of special short-to-medium-range ordered structures.

To understand the effect of the degree of structural order on the MCE in more detail, the change of the field dependence of $-\Delta S_M$ is analyzed. All the as-cast and annealed MGs show a second-order phase transition (SOPT), as can be indicated from the positive slope of the Arrott plots [39]. For magnetic materials with a SOPT, $-\Delta S_M^{max}$ and H are found to follow the formula [40]: $-\Delta S_M^{max} \propto H^n$, where n is an exponent of the field dependence of $-\Delta S_M^{max}$. The experimental data and the fitting curves are presented in Fig. 5(a). The exponents n for the as-cast MG and the MGs annealed at 578 K and 620 K for 60 min are 0.75, 0.77 and 0.76, respectively. The MG annealed at 578 K for 60 min has the largest n, showing the most sensitivity of $-\Delta S_M^{max}$ to external field change. The larger exponent n of the three alloys than 2/3 predicted by the mean field theory [41] may come from the inhomogeneous local structures in the MGs. In addition, after normalizing $-\Delta S_M$ and rescaling the temperature as following [42]:

$$\begin{cases} \Delta S^{*} = \Delta S_M / \Delta S_M^{max} \\ \theta = (T_C - T)/(T_{r1} - T_C), T < T_C \\ \theta = (T - T_C)/(T_{r2} - T_C), T \geq T_C \end{cases}$$

where T_{r1} and T_{r2} correspond to the temperature at half of the peak, the obtained $\Delta S^{*}(\theta)$ curves collapse well onto a single curve for the three MGs as shown in Fig. 5(b). This further confirms that these MGs exhibit

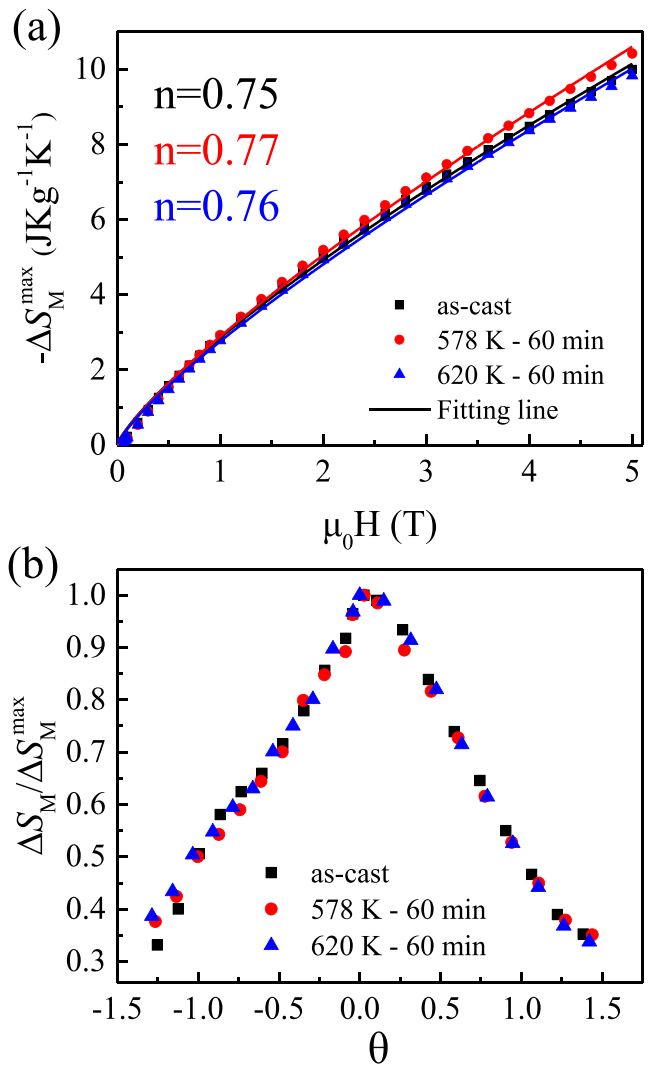

Fig. 5. (a) Extrapolation of the fitted data for the as-cast MG and MGs annealed at 578 and 620 K for 60 min according to the formula $-\Delta S_M^{max} \propto H^n$. (b) Universal curves of the as-cast MG and MGs annealed at 578 and 620 K for 60 min as a function of the rescaled θ .

SOPT and annealing does not cause crystallization and formation of the secondary phases. The universal curve in these alloys also implies that their critical exponents are the same and not sensitive to the degree of structure order.

In summary, we tuned MCE of $Gd_{55}Co_{20}Al_{24.5}Si_{0.5}$ bulk MG via controlling the degree of structural order. It is found that the degree of structural order plays a significant impact on the magnetocaloric performance of MGs. And large maximum magnetic entropy change of 10.8 ± 0.6 JKg^{-1}K^{-1} is obtained for the MG annealed at 536 K for 60 min, which is the highest value among the Gd-based MGs. Furthermore, the crystallization enthalpy, saturation magnetization and $-\Delta S_M^{max}$ of the annealed alloys have a good linear relationship with each other. These findings are of great significance to comprehend the nature of MCE in MGs and for the development of new amorphous systems with advanced magnetic performances.

Author contributions

Z.G. Zhang conducted sample preparation, performance testing, data processing and article writing. Q. Luo and B.L. Shen conceived the research and completed the manuscript. L.L. Shao and L. Xue conducted the annealing experiments. All authors contributed to data analysis and discussion.

Declaration of Competing Interest

The authors declare that they have no known competing financial interests or personal relationships that could have appeared to influence the work reported in this paper.

Acknowledgment

This work was supported by the National Natural Science Foundation of China (Grant Nos. 51971061, 51631003 and 51971160) and the Fundamental Research Funds for the Central Universities (Grant No. 2242020R1003).

Data Availability Statement

The data that support the findings of this study are available from the corresponding author upon reasonable request.

References

[1] O. Tegus, E. Bruck, L. Zhang, Dagula, K.H.J. Buschow, F.R. de Boer, Magnetic-phase transitions and magnetocaloric effects, Phys. B 319 (2002) 174–192.
[2] V. Provenzano, A.J. Shapiro, R.D. Shull, Reduction of hysteresis losses in the magnetic refrigerant $Gd_5Ge_2Si_2$ by the addition of iron, Nature 429 (6994) (2004) 853–857.
[3] P. Yu, N.Z. Zhang, Y.T. Cui, L. Wen, Z.Y. Zeng, L. Xia, Achieving an enhanced magneto-caloric effect by melt spinning a $Gd_{55}Co_{25}Al_{20}$ bulk metallic glass into amorphous ribbons, J. Alloy. Compd. 655 (2016) 353–356.
[4] J. Liu, T. Gottschall, K.P. Skokov, J.D. Moore, O. Gutfleisch, Giant magnetocaloric effect driven by structural transitions, Nat. Mater. 11 (7) (2012) 620–626.
[5] V. Franco, J.S. Blazquez, J.J. Ipus, J.Y. Law, L.M. Moreno-Ramirez, A. Conde, Magnetocaloric effect: from materials research to refrigeration devices, Prog. Mater. Sci. 93 (2018) 112–232.
[6] O. Tegus, E. Brück, K.H.J. Buschow, F.R. de Boer, Transition-metal-based magnetic refrigerants for room-temperature applications, Nature 415 (6868) (2002) 150–152.
[7] Q. Luo, D.Q. Zhao, M.X. Pan, W.H. Wang, Magnetocaloric effect in Gd-based bulk metallic glasses, Appl. Phys. Lett. 89 (2006), 081914.
[8] V.K. Pecharsky, K.A. Gschneidner, Magnetocaloric effect from indirect measurements: magnetization and heat capacity, J. Appl. Phys. 86 (1999) 565.
[9] H. Neves Bez, H. Yibole, A. Pathak, Y. Mudryk, V.K. Pecharsky, Best practices in evaluation of the magnetocaloric effect from bulk magnetization measurements, J. Magn. Magn. Mater. 458 (2018) 301–309.
[10] M.H. Phan, S.C. Yu, Review of the magnetocaloric effect in manganite materials, J. Magn. Magn. Mater. 308 (2) (2007) 325–340.
[11] N.S. Bingham, H. Wang, F. Qin, H.X. Peng, J.F. Sun, V. Franco, H. Srikanth, M. H. Phan, Excellent magnetocaloric properties of melt-extracted Gd-based amorphous microwires, Appl. Phys. Lett. 101 (2012), 102407.
[12] A.L. Greer, Metallic glasses, Science 267 (5206) (1995) 1947–1953.
[13] C.F. Sanchez-Valdes, P.J. Ibarra-Gaytan, J.L. Sánchez Llamazares, M. Avalos-Borja, P. Alvarez-Alonso, P. Gorria, J.A. Blanco, Enhanced refrigerant capacity in two-phase nanocrystalline/amorphous $NdPrFe_{17}$ melt-spun ribbons, Appl. Phys. Lett. 104 (2014), 212401.
[14] H. Fu, M. Zou, N.K. Singh, Modification of magnetic and magnetocaloric properties of Dy-Co-Al bulk metallic glass introduced by hydrogen, Appl. Phys. Lett. 97 (2010), 262509.
[15] H. Fu, Q. Zheng, M.X. Wang, Magnetocaloric effect contributed by in situ dual-phase structure in the Gd-Co-Al alloy, Appl. Phys. Lett. 99 (2011), 162504.
[16] Q. Zheng, L.L. Zhang, J. Du, Magnetic entropy change in $Gd_{95}Fe_{2.8}Al_{2.2}$ amorphous/nanocrystalline ribbons, Scr. Mater. 130 (2017) 170–173.
[17] S. Gorsse, B. Chevalier, G. Orveillon, Magnetocaloric effect and refrigeration capacity in $Gd_{60}Al_{10}Mn_{30}$ nanocomposite, Appl. Phys. Lett. 92 (2008), 122501.
[18] X.C. Zhong, H.Y. Yu, Z.W. Liu, R.V. Ramanujan, Influence of crystallization treatment on structure, magnetic properties and magnetocaloric effect of $Gd_{71}Ni_{29}$ melt-spun ribbons, Curr. Appl. Phys. 18 (11) (2018) 1289–1293.
[19] J.W. Lai, Z.G. Zheng, X.C. Zhong, V. Franco, R. Montemayor, Z.W. Liu, D.C. Zeng, Table-like magnetocaloric effect of $Fe_{88-x}Nd_xCr_8B_4$ composite materials, J. Magn. Magn. Mater. 390 (2015) 87–90.
[20] H.W. Sheng, W.K. Luo, F.M. Alamgir, J.M. Bai, E. Ma, Atomic packing and short-to-medium-range order in metallic glasses, Nature 439 (7075) (2006) 419–425.
[21] Y.H. Liu, D. Wang, K. Nakajima, W. Zhang, A. Hirata, T. Nishi, A. Inoue, M. W. Chen, Characterization of nanoscale mechanical heterogeneity in a metallic glass by dynamic force microscopy, Phys. Rev. Lett. 106 (2011), 125504.
[22] Y.Q. Cheng, E. Ma, Atomic-level structure and structure-property relationship in metallic glasses, Prog. Mater. Sci. 56 (4) (2011) 379–473.

[23] J. Ding, S. Patinet, M.L. Falk, Y. Cheng, E. Ma, Soft spots and their structural signature in a metallic glass, Proc. Natl. Acad. Sci. U. S. A. 111 (39) (2014) 14052–14056.
[24] M. Zhou, K. Hagos, H.Z. Huang, M. Yang, L.Q. Ma, Improved mechanical properties and pitting corrosion resistance of $Zr_{65}Cu_{17.5}Fe_{10}Al_{7.5}$ bulk metallic glass by isothermal annealing, J. Non-Cryst. Solids 452 (2016) 50–56.
[25] J.E. Gao, H.X. Li, Z.B. Jiao, Y. Wu, Y.H. Chen, T. Yu, Z.P. Lu, Effects of nanocrystal formation on the soft magnetic properties of Fe-based bulk metallic glasses, Appl. Phys. Lett. 99 (2011), 052504.
[26] Jan Świerczek, Nanocrystallization and magnetocaloric effect in amorphous Fe-Mo-Cu-B alloy, J. Alloy. Compd. 615 (2014) 255–262.
[27] Qiang Luo, Jun Shen, Tuning magnetocaloric effect of Gd-Er-Al-Co metallic glass through crystallization, J. Iron Steel Res. Int. 25 (6) (2018) 619–623.
[28] L. Xia, K.C. Chan, Enhanced magnetocaloric effect of a partially crystalline $Gd_{55}Al_{20}Ni_{25}$ bulk metallic glass, Solid State Sci. 13 (12) (2011) 2086–2089.
[29] Q.Y. Dong, B.G. Shen, J. Chen, J. Shen, F. Wang, H.W. Zhang, J.R. Sun, Magnetic properties and magnetocaloric effects in amorphous and crystalline GdCuAl ribbons, Solid State Sci. 149 (2009) 417–420.
[30] Q. Luo, B. Schwarz, N. Mattern, J. Shen, U. Eckert, Roles of hydrogenation, annealing and field in the structure and magnetic entropy change of Tb-based bulk metallic glasses, AIP Adv. 3 (2013), 032134.
[31] Q. Luo, W.H. Wang, Magnetocaloric effect in rare earth-based bulk metallic glasses, J. Alloy. Compd. 495 (1) (2010) 209–216.
[32] L. Xue, L.L. Shao, Q. Luo, L.N. Hu, Y.B. Zhao, K.B. Yin, M.G. Zhu, L.T. Sun, B. L. Shen, X.F. Bian, Liquid dynamics and glass formation of $Gd_{55}Co_{20}Al_{25}$ metallic glass with minor Si addition, J. Mater. Sci. Technol. 77 (2021) 28–37.
[33] C. Gammer, C. Mangler, C. Rentenberger, H.P. Karnthaler, Quantitative local profile analysis of nanomaterials by electron diffraction, Scr. Mater. 63 (3) (2010) 312–315.
[34] J.M. Liang, L.J. Chen, Autocorrelation function-analysis of phase-formation in the initial-stage of interfacial reactions of molybdenum thin-films on (111)Si, Appl. Phys. Lett. 64 (10) (1994) 1224–1226.
[35] G.Y. Fan, J.M. Cowley, Autocorrelation analysis of high-resolution electron-micrographs of near-amorphous thin-films, Ultramicroscopy 17 (4) (1985) 345–355.
[36] X.J. Liu, G.L. Chen, H.Y. Hou, X. Hui, K.F. Yao, Z.P. Lu, C.T. Liu, Atomistic mechanism for nanocrystallization of metallic glasses, Acta Mater. 56 (12) (2008) 2760–2769.
[37] V.M. Giordano, B. Ruta, Unveiling the structural arrangements responsible for the atomic dynamics in metallic glasses during physical aging, Nat. Commun. 7 (1) (2016), https://doi.org/10.1038/ncomms10344.
[38] T. Hashimoto, T. Numasawa, M. Shino, T. Okada, Magnetic refrigeration in the temperature range from 10 K to room-temperature: the ferromagnetic refrigerants, Cryogenics 21 (11) (1981) 647–653.
[39] S.K. Banerjee, On a generalized approach to 1st and 2nd order magnetic transitions, Phys. Lett. 12 (1964) 16–17.
[40] V. Franco, A. Conde, Scaling laws for the magnetocaloric effect in second order phase transitions: From physics to applications for the characterization of materials, Int. J. Refrig. 33 (2010) 465–473.
[41] H. Oesterreicher, F.T. Parker, Magnetic cooling near curie temperatures above 300 K, J. Appl. Phys. 55 (1984) 4334.
[42] V. Franco, J.S. Blazquez, A. Conde, Field dependence of the magnetocaloric effect in materials with a second order phase transition: a master curve for the magnetic entropy change, Appl. Phys. Lett. 89 (2006), 222512.
[43] C.M. Pang, L. Chen, H. Xu, W. Guo, Z.W. Lv, J.T. Huo, M.J. Cai, B.L. Shen, X. L. Wang, C.C. Yuan, Effect of Dy, Ho, and Er substitution on the magnetocaloric properties of Gd-Co-Al-Y high entropy bulk metallic glasses, J. Alloy. Compd. 827 (2020), 154101.
[44] L. Xue, L.L. Shao, Q. Luo, B.L. Shen, $Gd_{25}RE_{25}Co_{25}Al_{25}$ (RE = Tb, Dy and Ho) high-entropy glassy alloys with distinct spin-glass behavior and good magnetocaloric effect, J. Alloy. Compd. 790 (2019) 633–639.
[45] F. Yuan, J. Du, B.L. Shen, Controllable spin-glass behavior and large magnetocaloric effect in Gd-Ni-Al bulk metallic glasses, Appl. Phys. Lett. 101 (2012), 032405.
[46] J. Du, Q. Zheng, Y.B. Li, Q. Zhang, D. Li, Z.D. Zhang, Large magnetocaloric effect and enhanced magnetic refrigeration in ternary Gd-based bulk metallic glasses, J. Appl. Phys. 103 (2) (2008) 023918, https://doi.org/10.1063/1.2836956.
[47] J.T. Zhu, Q. Luo, M.J. Cai, B. Ji, B.L. Shen, Magnetocaloric performance and its linear relationship with magnetoresistance in Gd-Al-Cu metallic glass, J. Magn. Magn. Mater. 507 (2020), 166828.
[48] L. Xia, Q. Guan, D. Ding, M.B. Tang, Y.D. Dong, Magneto-caloric response of the $Gd_{60}Co_{25}Al_{15}$ metallic glasses, Appl. Phys. Lett. 105 (2014), 192402.
[49] Q.Y. Dong, B.G. Shen, J. Chen, J. Shen, F. Wang, H.W. Zhang, J.R. Sun, Large magnetic refrigerant capacity in $Gd_{71}Fe_3Al_{26}$ and $Gd_{65}Fe_{20}Al_{15}$ amorphous alloys, J. Appl. Phys. 105 (2009), 053908.
[50] B. Schwarz, B. Podmilsak, N. Mattern, J. Eckert, Magnetocaloric effect in Gd-based $Gd_{60}Fe_xCo_{30-x}Al_{10}$ metallic glasses, J. Magn. Magn. Mater. 322 (16) (2010) 2298–2303.